Arch. Metall. Mater., Vol. 61 (2016), No 2B, p. 933–936

DOI: 10.1515/amm-2016-0158

D. JAKUBOWSKA*, J. ZDUNEK*, M. KULCZYK**, J. MIZERA*, K.J. KURZYDŁOWSKI*

MICROSTRUCTURE EVOLUTION AND TEXTURE DEVELOPMENT IN A CU-8.5%AT. AL MATERIAL SUBJECTED TO HYDROSTATIC EXTRUSION

The aim of the present paper was to investigate microstructure and texture evolution of two single crystals and polycrystal of Cu-8.5%at.Al material. All of mentioned samples were deformed by HE to achieve true strain $\varepsilon = 1.17$. For microstructure analyzes observations by transmission electron microscope (STEM) were done. Crystalline size for samples after SPD were determine using XRD method. The global texture measurements were done using Bruker D8 Discover diffractometer equipped in Cr radiation. Microstructure investigations revealed nanocrystalline structure in single crystals with initial orientations <110> and <100> and polycrystalline Cu-8.5%at.Al material after SPD. The global texture measurements have shown the stability of initial orientation of <100> Cu-8.5%at.Al single crystal after HE, whereas the same SPD process strongly brakes up the orientation <110> Cu-8.5%at. Al single crystal.

Keywords: hydrostatic extrusion, texture, XRD, single crystal

1. Introduction

Severe Plastic Deformation (SPD) techniques have aroused great interest because of the possibility of achieving significant improvement in the mechanical and physical properties of the deformed materials [1-3]. In the case of metals and their alloys, this can be achieved in two ways: using the "bottom-up" technique or using the "top down" technique. The former technique is based on powder metallurgy, whereas the latter is used in severe plastic deformation methods. Hydrostatic extrusion (HE) is one of the SPD methods that induces ultra-fine grain structures in metals or alloys without contamination and internal porosity [4]. The most meaningful advantage of the HE process is that there is no friction between the billet and the container wall, and thus the length of the billet is not limited as it is in conventional extrusion. Furthermore, the frictional forces between the die and the billet tend to be lower in hydrostatic extrusion [5]. The working limit of this SPD process is set mainly by the fatigue strength of the container, and it is essential to be able to predict the extrusion pressure for each application [5]. The extrusion pressure is affected by geometrical factors such as extrusion ratio and die angle, the flow stress of the material, and the friction forces between die and billet [6]. At present, most of the available publications are focused on the effect of SPD on polycrystalline materials [7-10]. The authors of the present paper were concerned with investigating changes in single crystals and polycrystalline material subjected to SPD realized by HE. They found it interesting to compare the changes caused by HE realized on initial single crystals and polycrystals. The HE process on Cu-8.5%at.Al was not investigated before. In this paper, two single crystals of Cu-8.5%at.Al were examined with different primary orientations, as well as polycrystalline material of the same chemical composition.

2. Material and experiment

Cu-8.5% at. Al <110> and <100> (Fig. 1a and b) single crystals and Cu-8.5%at.Al polycrystalline alloy (Fig. 1c) with a low Stacking Fault Energy (SFE) (<10 mJ/m^2) were used for extrusion. The samples were cut using a spark erosion saw, and all samples before HE (both single crystals and polycrystal) were cylindrical in shape with a diameter of Φ9 and a length 50 mm. Hydrostatic extrusion was carried out at room temperature in two steps (from Φ9 mm to Φ7 mm and then to Φ5 m, which corresponds to total strain of 1.17). During the extrusion, the <100> and <110> directions were perpendicular to the extrusion direction (ED), as shown in Fig. 2. A total strain introduced by the processing is defined by the relationship of the billet and product diameters (Φ and ϕ, respectively):

$$\varepsilon = 2 \ln \frac{\Phi}{\phi}$$

* WARSAW UNIVERSITY OF TECHNOLOGY, MATERIALS SCIENCE AND ENGINEERING FACULTY, POLAND
** INSTITUTE OF HIGH PRESSURE PHYSICS, POLISH ACADEMY OF SCIENCES (UNIPRESS), WARSAW, POLAND

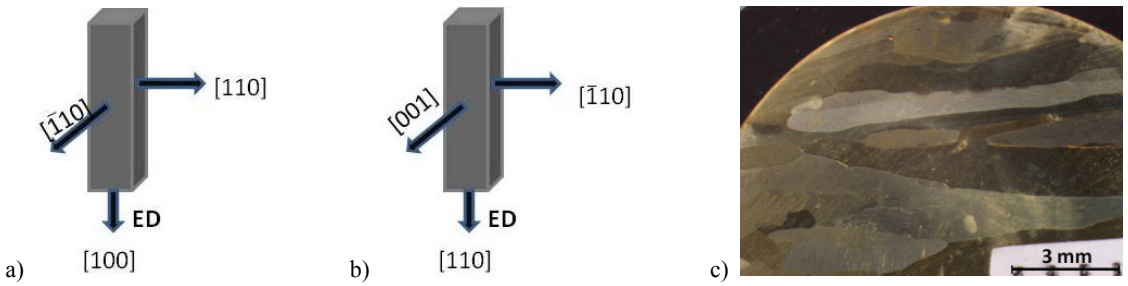

Fig. 1. Samples before the deformation process: schematic representation of the orientation of single crystals a) and b), and microstructure of polycrystalline Cu-8.5% at.Al alloy on a surface perpendicular to the extrusion direction c)

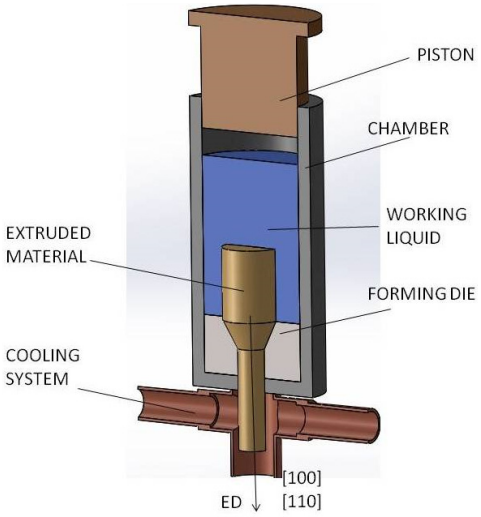

Fig. 2. The scheme of hydrostatic extrusion

The changes in mechanical properties were observed by measuring microhardness on a section perpendicular to the extrusion direction in samples before and after HE. The microhardness was measured using a ZWICK microhardness tester equipped with a microscope that permitted the precise measurement of the indentation diagonal. The global texture measurements were made using the Bruker D8 Discover X-ray diffractometer at planes perpendicular to the extrusion direction, applying filtered Cr $K\alpha$ radiation ($K\alpha_1$ = 0.228 nm). On the basis of the measured pole figures, the Orientation Distribution Functions (ODF) were computed for each sample, and then a quantitative assessment of the shares of major texture components was made. In the state after deformation, the microstructure was examined using a JEOL 1200 transmission electron microscope (TEM). To obtain a complete characterization of the micstrostructure after HE, the crystalline size was measured using a Bruker D8 Da Vinci Advance equipped with Cu radiation.

The microstructure and texture of the polycrystalline material were analysed before hydrostatic extrusion. The mean grain size d_2 (defined as the diameter of the circle that has a surface area equal to the surface area of a given grain) for polycrystalline Cu-8.5%at. Al was d_2 = 1.2 mm. The texture measurements on initial polycrystalline material revealed the presence of two main texture components, <110> and <100>, with different volume fractions (Table 1).

3. Results and discussion

The microstructures of all deformed samples are shown in Figure 3. The analyses of the received STEM images led to the same conclusions as for deformed single crystals and polycrystals. The domination of a band microstructure is observed, and there are deformation twins inside those bands. Most grains are elongated to the direction of band propagation. For determining crystalline size, XRD measurements were conducted using the Williamson-Hall method (Fig. 4). In all of the deformed samples, a nanocrystalline structure was observed. The analysis of crystalline size yields both twin thickness and grain size measurements. This nanocrystalline structure is typical for materials

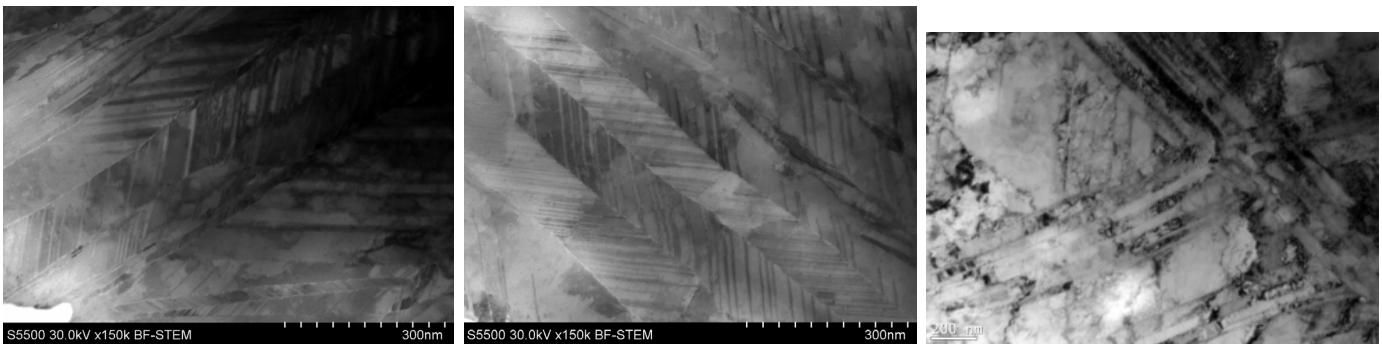

Fig. 3. Microstructure of Cu-8.5% at. Al: a) <110> and b) <100> single crystals, and c) polycrystals after HE ε = 1.17

with low SFE [11-12]. This type of structure in deformed Cu-Al polycrystalline materials with different SFE was also observed by S. Qu et al. [13]. By taking into account the observation that minimum grain size decreases by lowering SFE, the authors concluded that the grain sizes of Cu-Al alloys may be controlled by the value of SFE. They examined the Cu-8%at.Al alloy after 1-4 equal-channel angular pressing (ECAP), and they achieved an effective strain of ~1.15 in the first pass. For samples after one ECAP pass, the effective strain was comparable to that of the samples investigated in this paper after HE, which developed a homogeneous, nanocrystalline structure with deformation bands with deformation twins inside it. The authors concluded that it is easier to obtain the homogeneous microstructure in Cu-Al alloys than in materials with medium SFE. X.H.An et al. [14] also examined Cu-Al alloys with different volume fractions of Al after ECAP. They mentioned that the addition of Al lowers the SFE, changing the dislocation activities and simplifying deformation twining. They summarized that the addition of elemental Al combined with the deformation achieved by ECAP increased the hardness and ductility values. Simultaneous enhancement of strength and ductility strongly depend on deformation twins and their intersections.

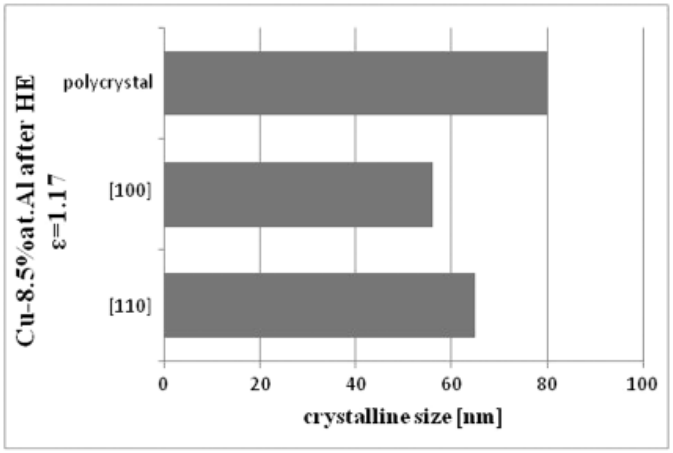

Fig. 4. Crystalline size of samples after HE $\varepsilon = 1.17$

The HV1 microhardness of samples in the initial state and after deformation was measured on the section perpendicular to the extrusion direction. Figure 5 compares the microhardness of polycrystalline Cu-8.5%at. Al with the two single crystals (<100> and <110>) in both the initial state and after HE. The comparison indicates that both the deformed single crystals and the polycrystals have comparable microhardness values and that their mechanical properties do not depend on the starting orientation/texture of the material.

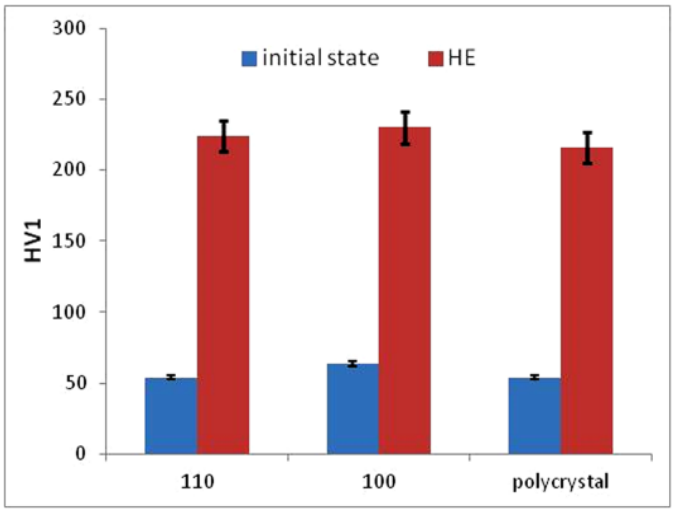

Fig. 5. Comparison of the microhardness of polycrystalline Cu-8.5%at. Al and the two single crystals <110> and <100> in the initial state and after HE

XRD measurements were conducted for qualitative and quantitative (Table 1) texture analyses. The received pole figures revealed the fibrous texture in samples after severe plastic deformation from the hydrostatic extrusion process (Fig. 6). The XRD measurements were conducted on a plane perpendicular to the extrusion direction (ED). Due to the grain size of polycrystalline materials before the deformation, XRD measurements were conducted at several points on the sample.

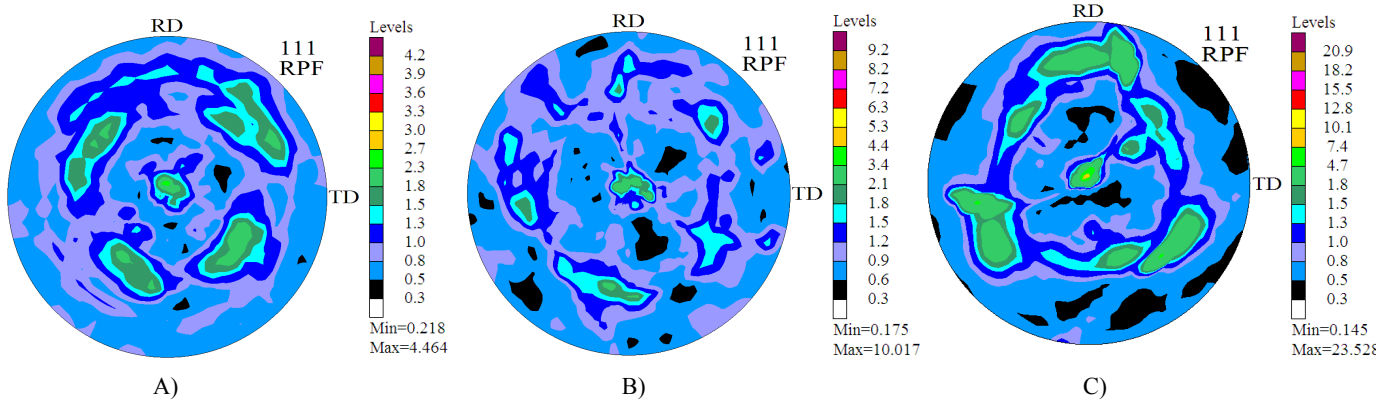

Fig. 6. {111} pole figures for Cu-8.5%at. Al single crystals after the hydrostatic extrusion process, with initial orientations of A) <110>, B) <100>, and C) polycrystal

TABLE 1

Volume fraction of texture components of the Cu-8.5%at. Al materials deformed by HE

Orientation/texture of Cu-8.5%at.Al, Volumetric content of the component V [%]		
linitial state		**after HE ε=1.17**
single crystal	<100>	<111>16% <100>19% background 65%
	<110>	<100> 8% background 92%
polycrystal	<100> 33% <110> 21% background 46%	<111>17% <114> 19% background 64%

The analysis of texture after HE revealed the instability of the original orientation of the <110> single crystal. This is in contrast with the texture of the <100> single crystal, where the initial orientation was preserved in one fifth of the volume fraction. The extruded polycrystals and single crystal with an initial orientation of <100> have an identical texture component: fibrous <111> with a comparable volume fraction. Our results are in agreement with the conclusion reported by Wróbel et al. [11], who investigated a Cu-Al single crystal deformed by cold rolling. One of their conclusions was that Cu-Al with a [110] orientation breaks up during rolling into deformation bands.

Some results [12,13] show that relatively equal amounts of <111> and <100> components are produced in uniaxially deformed fcc materials. English and Chin [12] showed that the strength of the <100> component decreases with increasing SFE. This is assigned to mechanical twinning. The orientations near <111> will twin first because the resolved shear stress for twinning is highest [14]. The texture formation in low SFE materials can also be explained because of the easy formation of twins, so all orientations can form twins.

4. Summary

Experiments were conducted to determine changes in single crystalline and polycrystalline Cu-8.5%at. Al after HE $\varepsilon = 1.17$. The main conclusions are as follows:

- Nanocrystalline structure, which was full of deformation twins, was achieved both in deformed Cu-8.5%at. Al polycrystals and in single crystals.
- The severe plastic deformation realized by HE $\varepsilon = 1.17$ brought about strong breaks in the original texture of the <100> single crystal, whereas the initial texture of the <110> single crystal was preserved in 19% of the sample.

Acknowledgements

This work was supported in part by the National Centre of Science in Poland, Project no:2013/09/B/ST8/03754

REFERENCES

[1] R.Z. Valiev, R.K. Islamgaliev, I.V. Alexandrov, Bulk Nanostructured Materials from Severe Plastic Deformation, (2000).
[2] M. Kulczyk, W. Pachla, A. Mazur, R. Diduszko, H. Garbacz, M. Lewandowska, W. Łojkowski, K.J. Kurzydłowski, Sci. Mater. **23** (2005).
[3] A. Zhilyaev, B.-K. Nurislamova, M. Kim, Baró, J. Szpunar, T. Langdon, Acta Mater. **51**, 753 (2003).
[4] A. Mishra, B. Kad, F. Gregori, M. Meyers, Acta Mater. **55**, 13 (2007).
[5] N. Inoue, M. Nishihara, Hydrostiatc Extrusion. Theory and Applications, (1985).
[6] S. Zherebtsov, A. Mazur, G. Salishchev, W. Lojkowski, Mater. Sci. Eng. **A 485**, 39 (2008).
[7] W. Pachla, J. Skiba, M. Kulczyk, S. Przybysz, M. Przybysz, M. Wróblewska, R. Diduszko, R. Stepniak, J. Bajorek, M. Radomski, W. Fafara, Mater. Sci. Eng. **A 615**, 116 (2014).
[8] J. Bohlen, S.B. Yi, J. Swiostek, D. Letzig, H.G. Brokmeier, K.U. Kainer, Scr. Mater. **53**, 259 (2005).
[9] W. Chrominski, M. Kulczyk, M. Lewandowska, K.J. Kurzydlowski, Mater. Sci. Eng. **A 609**, 80 (2014).
[10] P. Bazarnik, M. Lewandowska, K.J. Kurzydłowski, Arch. Metall. **57**, 869 (2012).
[11] S. Dymek, M. Wróbel, Mater. Chem. Phys. **81**, 552 (2003).
[12] A.T. English, G.Y. Chin, Acta Met. **13**, 1013 (1965).
[13] H. Wenk, Preferred Orientation in Deformed Metals and Rocks: An Introduction to Modern Texture Analysis, Elsevier, 22.10.2013 – 610, (1985).
[14] B. Verlinden, J. Driver, I. Samajdar, Thermo-Mechnical Processing of Metalic Materials **11**. Pergamon Materials Series (2007).